

Phase Shift Modulation Strategy for Single Stage AC to DC Dual Active Bridge Converter

Maha Faiz Ahmed*, Mohamad N. Abdul Kadir

Electrical Engineering Department, Collage of Engineering, University of Mosul, Mosul, Iraq

Correspondance

*Maha Faiz Ahmed

Electrical Engineering Department,

Collage of Engineering,

University of Mosul, Mosul, Iraq

Email: mahaalqazzaz@gmail.com

Abstract

Energy exchange between AC grid and DC supply that is a part of a hybrid electric micro-grid takes place using various power converter designs. The single-phase, single-stage, AC-DC power dual active bridge converter is one option. The phase-shift modulation is used to regulate energy flow in both directions. The topology of one stage AC-DC dual active bridge converter based in bidirectional switching modules has been introduced. This paper next introduces the analysis of the AC side current considering basic modulation functions and suggests an optimum phase-shifted modulation strategy. The proposed modulation function provides minimum harmonics distortion. A simulation study is presented to compare the proposed strategy to the basic sinusoidal and triangular modulation techniques. The results show that the modified modulation reduces the average THD by about 55% and 39% compared to the standard sinusoidal and triangular modulation strategies respectively and ensures linear relationship between the transferred power and magnitude control coefficient.

Keywords

Dual active bridge, Phase shift modulation, Trapezoidal modulation, Time harmonic distortion, Triangular modulation.

I. INTRODUCTION

Renewable energy sources like wind, solar, hydropower, and others are increasingly used to meet the rising demand of electricity. Green energy sources must be integrated with the traditional electric power system using power electronic converters [1]. The integration of these sources with the traditional electric power grid poses significant challenge in terms of energy quality [2].

Different converter topologies and modulation strategies are used to control the power flow. The dual active bridge (DAB) receives attention for its important features such as isolation, high power density, bidirectional power flow capability. Based on shifting the phase of the voltages applied to the high-frequency transformer terminals of the power converter, the phase-shift modulation (PSM) approach regulates the bidi-

rectional transmission of power. This tactic is used in [3,4] for DC-DC converters and DC-AC converters, respectively. Given that the AC voltage amplitude changes during the grid interval for a DC-AC converter, PSM with continuously variable phase-shift is used in this case [5].

Besides the PSM, other control methods are also used to control DAB converters. In trapezoidal modulation (TZM) and triangular modulation (TRM) methods the bridge converters are operated in quasi square wave mode [6]. A mix of the TZM and TRM methods to lower power losses within a particular working range for a DC-DC converter is presented in [7]. These techniques use the DC-DC converter to create a trapezoidal or triangle pattern for the current passing through the high-frequency transformer. A mixed modulation strategy based on PSM, TZM, and TRM strategies is proposed in [8] and applied to a DC-DC converter for ultracapacitor uses to



This is an open-access article under the terms of the Creative Commons Attribution License, which permits use, distribution, and reproduction in any medium, provided the original work is properly cited.
©2024 The Authors.

Published by Iraqi Journal for Electrical and Electronic Engineering | College of Engineering, University of Basrah.

increase the control range to lower power level.

Novel modulation scheme for a DC-DC converter is described in [9]. With the help of this scheme, you can choose a particular mode of operation to create the least amount of copper and conduction losses by driving the least amount of RMS current through the inductor. The PSM, TZM, and TRM modulation strategies are mixed in [10] in order to improve efficiency over a broad spectrum of DC-DC converter function. A dual-phase-shift modulation strategy is suggested in [11] to reduce reactive power in the DC-DC converter. However, it is not easy to switch between the various modulation methods used with the DC-DC converter. As a result, [12] presents a straightforward and adaptable idea for creating pulse width modulation signals for all potential modulation techniques. The modulation technique described in [13] regulates the single-phase DC-AC converter under soft switching for the working range in internal mode and yields an AC side current with a power factor (PF) that is nearly 1. To produce a current with a low THD and PF close to 1 on the AC side, a combined phase-shift and frequency modulation is employed in an isolated, bidirectional single-phase DC-AC converter. The soft-switching operation range is used to carry out this procedure [14]. A sinusoidal pulse width modulation is used to produce an AC side current with PF near to 1 and lower THD in order to increase the soft-switching operation range within a specific range of power transferred [15]. When the modulated voltages applied to the high-frequency transformer terminals of the power converter reach a 50 percent duty cycle and a 90° phase angle between them, the operation point at which the highest power is obtained [5, 15]. Because the overall harmonic distortion of the current has increased, the papers listed above do not assess the single-phase single-stage isolated AC-DC converter at the working point where the maximum power can be transferred. Taking into account the operating position for optimal power transmission. The modified phase-shift modulation strategy proposed in [16] allows controlling the power transferred and obtain a PF close to 1 and an AC current with lower harmonic distortion (THDi) for entire operation range of the isolated single-phase single-stage DC-AC converter.

When converting from DC to AC in [7], one approach is to use DC-DC converter first, which utilizes a separate DC bus and capacitors. The size and cost of these capacitors can vary [8]. Otherwise, there are a variety of configurations that perform DC-AC conversion in an isolated and bidirectional manner without the need for a DC-DC conversion step [9–15]. The designs known as solid-state transformers (SST) [6, 17] are frequently used with these separated and bidirectional DC-AC converters.

The aim to this study is to develop a single stage AC-DC, DAB converter with a modulation scheme to minimize the

THD of the AC side current. The approach of this study is based on two phases: design and verification. In design phase, the converter circuit is suggested and AC current is analyzed to develop the modulation function. In verification phase, the performance of the system is studied using simulation platform.

In this paper the single-phase single-stage isolated DAB AC-DC converter has been presented. The AC side converter is based on bidirectional switching modules. The converter is controlled by PSM using different modulations functions sinusoidal, triangular and a new modified modulation function mPSM. The modified function that has been optimized for minimum THD. The function is derived assuming a pure sinusoidal AC current and it has been shown that it provides minimum harmonic distortion and decoupled active and reactive power control. This paper is organized as follows: Section II. presents the converter circuit and defines the switching states. Section III. presents the current equation of the PSM controlled converter and derives the current function for the basic modulation methods and the suggested a modified PSM method. Section IV. presents the simulation model and the results and Section V. gives the conclusions.

II. THE AC-DC CONVERTER CIRCUIT AND SWITCHING STATES

The single-phase single-stage AC-DC power converter shown in Fig. 1 used to link a DC bus source to a standard single-phase AC grid. The voltage of the single-phase AC grid is given by:

$$v_{ac}(t) = V_{ac,p} \sin \omega_o t \quad (1)$$

where $V_{ac,p}$ is the peak of the AC voltage, $\omega_o = 2\pi f_o = 2\pi/T$ is the grid frequency in Hz and T is the grid period in seconds. As shown in Fig.1 the AC side converter is similar to the standard H-bridge but it uses bidirectional switching modules, instead of single switching device. A single MOSFET cannot block AC voltage. To construct a 4-quadrant switching module, two anti-series connected devices are used. Common source and common drain configurations are possible. The former option is considered as it requires one gate drive for both MOSFETs. The reversible power flow management and isolation of grid from the DC bus is achieved through the high-frequency transformer.

The high frequency transformer, two H-bridges, and auxiliary inductance L_a used in this converter serve as an interface to join the DC and AC circuits.

The voltage between the terminals b and b' is imposed by the DC H-bridge. While the bidirectional AC H-bridge imposes the voltage between terminals a and a'. The basic idea behind how converters work is to regulate power transmission by

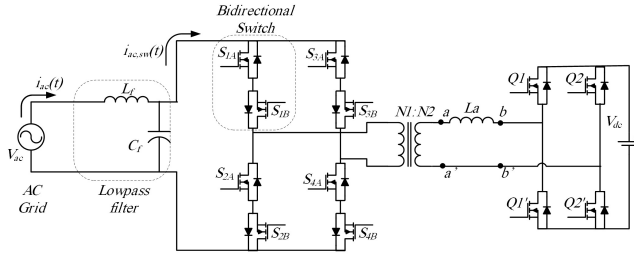


Fig. 1. The single-phase single-stage AC–DC power converter.

applying a phase shift between the modulated voltages $v_{aa'}$ and $v_{bb'}$. The inductor voltage, ($v_{La} = v_{aa'}v_{bb'}$), determines the power flow between the AC and DC sides.

The transformation ratio is defined as $n = N_2/N_1$, where N_1 and N_2 represent the number of winding turns on the AC side and DC side, respectively. A low-pass filter must be used to reduce the harmonic components that the commutations in the power devices cause i.e. in the AC grid current $i_{ac}(t)$ [18]. The AC filter has been designed according to the description given in previous work for similar filters [19].

In the AC H-bridge, each bidirectional switch is accomplished using two unidirectional switches, denoted by the letters S_{XA} and S_{XB} , respectively. The DC H-bridge switches are denoted by the symbol Q_X , where X is the switch number. The switching states and the resultant voltages are defined as shown in Table I. In this paper only PSM is applied, the switching states that produce zero output voltages have not been listed in this table.

In the AC H-bridge, each bidirectional switch is accomplished using two unidirectional switches, denoted by the letters S_{XA} and S_{XB} , respectively. The DC H-bridge switches are denoted by the symbol Q_X , where X is the switch number. The switching states and the resultant voltages are defined as shown in Table I. In this paper only PSM is applied, the switching states that produce zero output voltages have not been listed in this table.

III. PHASE-SHIFT MODULATION FUNCTIONS AND CURRENT EQUATIONS

This part shows a modulation strategy, which consists in switching the power devices of both H-bridges in order to impose a voltage nV_{Prim} between the terminals a and a' and the voltage $v_{bb'}$ both with a duty cycle of 50% and constant frequency. The phase shift is measured as the delay of the switching instant of the DC bridge with reference to AC bridge. Based on the assumption that the switching frequency is much higher than the AC line frequency, the AC line voltage is ap-

TABLE I.
SWITCHING STATES AND THE CORRESPONDING VOLTAGES

| vac | S_{1A} S_{4A} | S_{1B} S_{4B} | S_{2A} S_{3A} | S_{2B} S_{3B} | Q1 | Q2 | v_{La} $= v_{aa'}v_{bb'}$ |
|-----|----------------------|----------------------|----------------------|----------------------|----|----|--------------------------------|
| +ve | 1 | 1 | 0 | 1 | 1 | 0 | $nv_{ac} - Vdc$ |
| | | | | | 0 | 1 | $nv_{ac} + Vdc$ |
| | 0 | 1 | 1 | 0 | 1 | 0 | $-nv_{ac} - Vdc$ |
| | | | | | 0 | 1 | $-nv_{ac} + Vdc$ |
| -ve | 1 | 1 | 0 | 0 | 1 | 0 | $nv_{ac} - Vdc$ |
| | | | | | 0 | 1 | $nv_{ac} + Vdc$ |
| | 0 | 1 | 1 | 1 | 1 | 0 | $-nv_{ac} - Vdc$ |
| | | | | | 0 | 1 | $-nv_{ac} + Vdc$ |

proximately constant during a switching cycle. The average power transmission and the current waveform of the AC grid can be modified in accordance with the variation of phase shift [20]. The switching frequency defined as:

$$\omega_{sw} = 2\pi f_{sw} = 2\pi/T_{sw} \quad (2)$$

where f_{sw} is the switching frequency in Hz, and T_{sw} is the switching period in seconds. When both AC and DC converters are operated in square wave mode at f_{sw} and the phase shift angle δ is defined as the delay angle of the secondary switching compared to the primary. The power flow transferred between the AC side and the DC side is determined by δ . For $\delta > 0$ the power transfer is made from the AC side to DC side; alternatively for $\delta < 0$ where the power transfer is made from the DC side to the AC side. Fig. 2 shows a typical waveforms in a switching period of the voltages $v_{aa'}$ and $v_{bb'}$, the inductor voltage and current and the power transferred to the DC side. In this figure the converter losses are neglected and the power transferred is determined as the DC side voltage times current. A quantitative model based on the waveform of the instantaneous current through L_a can be used to infer the behavior of the converter as follows [21].

The series inductor, L_a , allows bidirectional power flow and controls the amount of power exchanged between the AC and DC sides. By changing the phase shift angle (δ), the subintervals of various voltage levels across the inductor changes which shapes the inductor current waveform. This current together with the switching state of the DC bridge, determine the average current of the DC source and hence the power transferred. The expression of the current in L_a , are defined by:

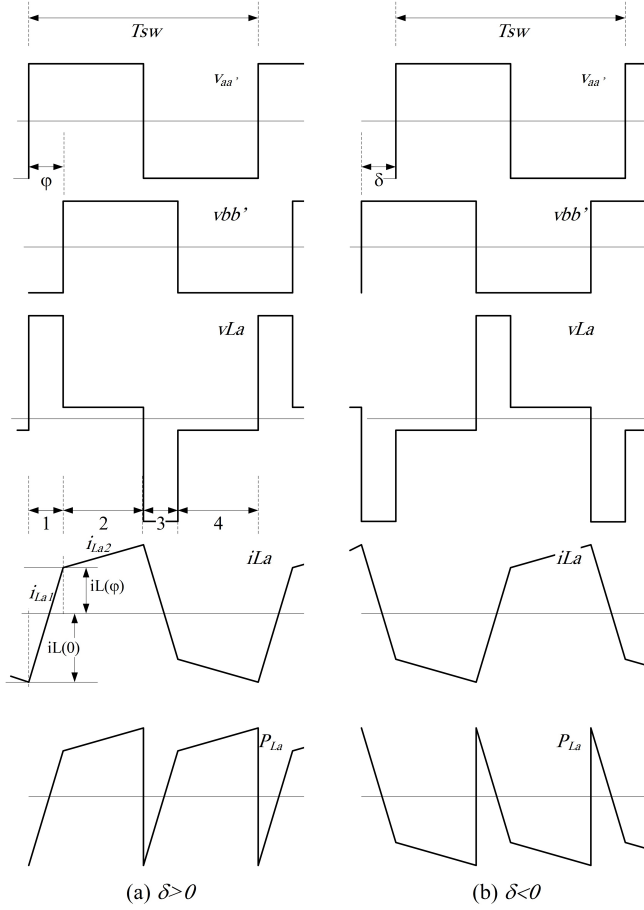


Fig. 2. Voltage and current waveforms over a switching period.

$$i_{La1}(t) = \frac{1}{\omega_{sw}L_a} \int_0^{\delta} v_{La} d\omega_{sw}t \quad (3)$$

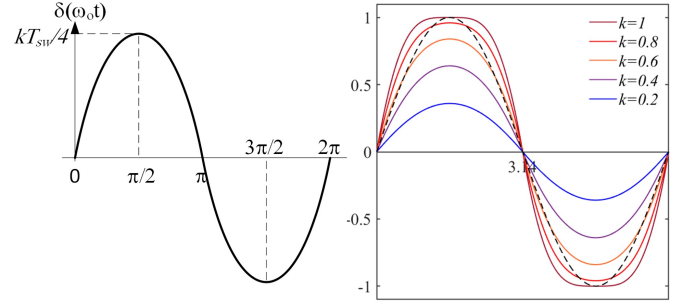
$$= \frac{nv_{prim} - v_{sec}}{L_a \omega_{sw}} \omega_{sw}t + i_{La}(0)$$

$$i_{La2}(t) = \frac{1}{\omega_{sw}L_a} \int_{\delta}^{\pi} v_{La} d\omega_{sw}t \quad (4)$$

$$= \frac{nv_{prim} - v_{sec}}{L_a \omega_{sw}} (\omega_{sw}t - \delta) + i_{La}(\delta)$$

where v_{La} is the voltage applied to terminals and $i_{La}(0)$ and $i_{La}(\delta)$ are the initial currents applied in L_a for intervals 1 and 2, respectively. The initial currents values can be obtained by:

$$i_{La}(0) = -\frac{nv_{prim} - v_{sec}}{2\omega_{sw}L_a} (\pi - \delta) - \frac{nv_{prim} - v_{sec}}{2\omega_{sw}L_a} (\delta) \quad (5)$$



(a) Modulation function (b) AC current

Fig. 3. Normalized current waveforms for different values of k using sinusoidal modulation.

$$i_{La}(\delta) = -\frac{nv_{prim} - v_{sec}}{2\omega_{sw}L_a} (\pi - \delta) + \frac{nv_{prim} - v_{sec}}{2\omega_{sw}L_a} (\delta) \quad (6)$$

In addition, current $i_{bac}(t)$ is a reflection of $i_{La}(t)$ current affected by the transformation ratio n and inverted by the switching sequence established. Therefore, in the intervals corresponding to 1-2 and 3-4, $i_{bac}(t)$ current presents the same waveform as can be observed in Fig. 3.

The average value of the AC converter current in a switching period can be deduced from:

$$i_{ac,sw} = n \frac{1}{\pi} \int_0^{\pi} i_{bac}(t) d\omega_{sw}t$$

$$= n \frac{1}{\pi} \left(\int_0^{\delta} i_{La1}(t) d\omega_{sw}t + \int_{\delta}^{\pi} i_{La2}(t) d\omega_{sw}t \right) \quad (7)$$

$$i_{ac,sw} = n \frac{V_{dc}}{L_a \pi \omega_{sw}} \delta (\pi - \delta)$$

According to (7), the value of $i_{ac,sw}$ during each commutation period depends on the system parameters and is a function of the variable phase shift angle δ . Therefore, it can be deduced that the current waveform during a grid period can be controlled by means of δ variation during different time intervals. The phase shift variation over the AC voltage period is defined by the modulation function. On the other hand, the waveform of $i_{ac}(t)$ current and the waveform of synthesised $i_{ac,sw}$ current in a grid period can be considered the same. With the aim of performing a theoretical analysis of the waveform of $i_{ac}(t)$ in a grid period using different modulation functions to operate the power converter, (7) can be normalized as shown in (8) when taking into account the following considerations that $nV_{dc}/L_a \pi \omega_{sw} = 1$, $f_1(t) = \delta(t)\pi$ and $f_2(t) = \delta(t)^2$, gives:

$$i_{ac}(t) = f_1(t) - f_2(t) \quad (8)$$

The following subsections describe the three modulation functions adopted in this paper. It has been considered that the

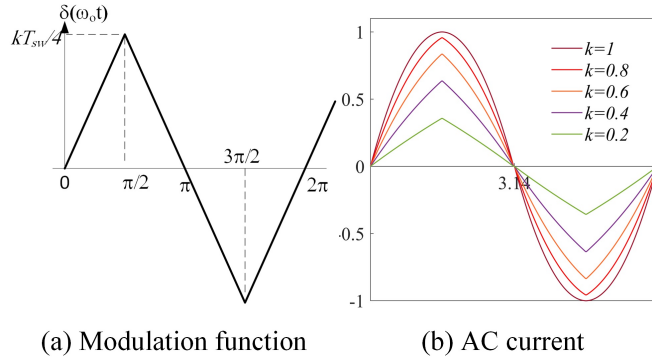


Fig. 4. Trigonometric modulation function and corresponding AC current.

aim is to produce a sinusoidal AC supply current with unity power factor.

A. Sinusoidal Modulation Function

The sinusoidal modulation function is shown in Fig. 3. Over the supply voltage period, the phase shift changes sinusoidal with the phase angle to reach it peak at $\omega_o t = \pi/2$. The peak value of the delay is equivalent to a quarter switching cycle when $k = 1$. The corresponding normalized current waveforms for different values of k are shown in Fig. 3. This figure shows that the current waveform becomes more distorted as k increases. A pure sine wave is shown Fig. 3 in broken line for waveform comparison.

B. Triangular Modulation Function

The triangular modulation function is shown in Fig. 4. Over the supply voltage period, the phase-shift changes linearly with the phase angle to reach it peak at $\omega_o t = \pi/2$. The peak value of the delay is equivalent to $(kT_{sw}/4)$, where power k is the control coefficient ($-1 < k < +1$). Normalized current waveforms for different values of k has been calculated using (8) and shown in Fig. 4. This figure shows that the current waveform becomes highly distorted as k decreases.

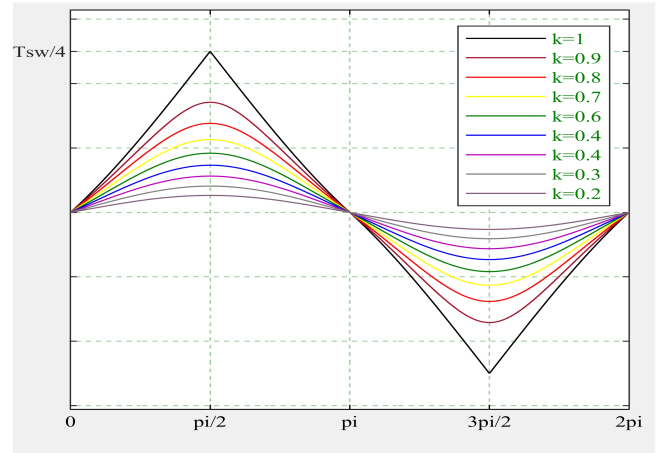
C. Modified Modulation Function

Aiming for minimum current distortion a special modulation function has been developed in this paper. The function is obtained from the solution of (7) for pure sinusoidal reference current $i_{ac}(t)^*$ given for unity power factor by:

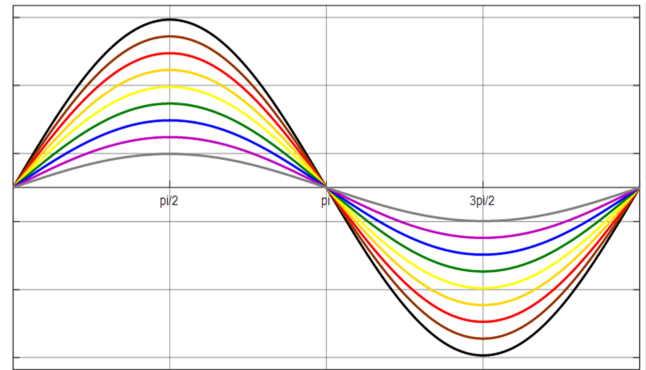
$$i_{ac}(t)^* = kI_{max,p} \sin(\omega_o t)$$

The modulation function is evaluated by solving (7) is given by:

$$\delta_{mod}(k, \omega_o t) = \frac{\pi - \sqrt{\pi^2 - 4kI_{max,p} \sin(\omega_o t)}}{2} \quad (9)$$



(a) Modulation function.



(b) AC current.

Fig. 5. The modified modulation function.

$$\delta_{mod}(k, \omega_o t) = \frac{\pi + \sqrt{\pi^2 - 4kI_{max,p} \sin(\omega_o t)}}{2} \quad (10)$$

Equations (9) and (10) are equivalent since the resultant angles are symmetrical around $\pi/2$, however (9) is used in order to keep the shift angle in the range $[-\pi/2 < \delta < \pi/2]$.

The resultant mPSM is shown in Fig. 5 for different values of k . Over the supply voltage period, the phase shift changes with the phase angle to reach it peak at $\omega_o t = \pi/2$. The peak value of the delay depends on k and equivalent to $\omega_o t = \pi/4$ when $k=1$. The modulation has different patterns depends on k , however the corresponding current waveform is always sinusoidal as shown in Fig. 5. This figure shows that the current waveform are sinusoidal regardless the value of k .

IV. SIMULATION AND RESULTS

The bidirectional AC-DC converter system has been evaluated by SIMULINK modelling using the parameters given in Table

TABLE II.
PARAMETERS OF THE BIDIRECTIONAL AC-DC
CONVERTER.

| Part | Parameters |
|-------------------|--|
| AC supply | 220V , 50Hz |
| AC filter | Cutoff frequency, $f_c = 2.5kHz$, Series inductance $L_f = 0.2mH$, with ESR, $r_L = 0.4\Omega$. Parallel capacitor, $C_f = 47\mu F$, with ESR, $r_C = 10m\Omega$ |
| AC side converter | Bidirectional switch module using two common source MOSFETs. MOSFET parameters: $R_{on} = 0.1\Omega$, $L_{on} = 0$, $R_d = 0.01\Omega$, $V_F=0$, $R_s = 1e5\Omega$ |
| Transformer | Linear transformer, Turn ratio=1, Fer-rite Core, $F=10kHz$, 5 KVA. |
| Series Inductor | $L_a = 0.15mH$ |
| DC side converter | The mosfet parameters: No. of bridge arms=2, $R_s = 1e5\Omega$, $R_{on} = 1e-3\Omega$ |
| DC supply | 350 V |

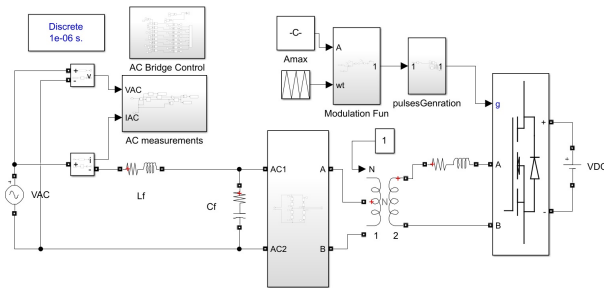


Fig. 6. The simulation model of the bidirectional AC-DC converter system.

II. The simulation model is shown in Fig. 6 with the AC side bridge converter drawn as one block. The "AC bridge control" block produces the switching signals of the AC bridge according to the polarity of the AC supply as described in Table I. The modulation function imposes a variable phase shift on DC side bridge. The resultant switching signals for the two converters over the grid voltage cycle are shown in Fig. 7. At the lower part of Fig. 7 a time zoom-in for the switching signals S_{1a} and Q_1 near $\omega t \approx 0$ and $\omega t \approx \pi/2$ are given to show the effect of phase-shift modulation.

A. Converter Operation in Sinusoidal Modulation

The converter controlled with sinusoidal modulation has been simulated with three values of reference power: 4500W, 3500W and 2500W. The waveforms of the resultant $i_{ac}(t)$ and the instantaneous current is shown in Fig. 8. It can be noticed that the current is highly distorted when $P=4500W$, for lower values of power the THD decreases, However, at very low

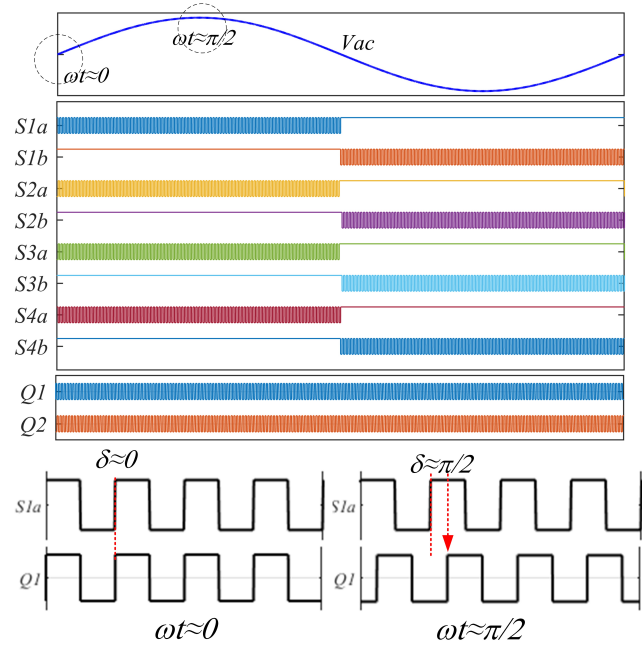


Fig. 7. The switching signals of the AC side and DC side converter as produced by the control blocks.

values of power the THD increases due to large distorting component of the voltage.

B. Converter Operation in Triangular Modulation

The simulation results of the AC current and instantaneous power of the converter operating with triangular modulation function and with three values of reference power: 4500W, 3500W and 2500W are shown in Fig. 9. It can be noticed that when the at output power of 4500W, i.e. k is close near 1, the current distortion is very low, however the distortion increases considerably at low power range.

C. Converter Operation in mPSM

The converter controlled with mPSM has been simulated with the same values of reference power used for other modulation functions. The waveforms of the resultant $i_{ac}(t)$ and the instantaneous power are shown in Fig. 10. It can be noticed that the current distortion is very low, except for small values of power due to large distorting voltage component.

D. Comparison Between the Three Modulation Methods

Figures 11, 12, and 13 show the response of the converter controlled with the three modulation methods when the magnitude control ratio (k) changes from 0.3-to-1.0. The power variation versus k is shown in Fig. 11. It can be shown that the suggested mPSM has the advantage of linear relationship between the power and k . Nevertheless, this method has smaller

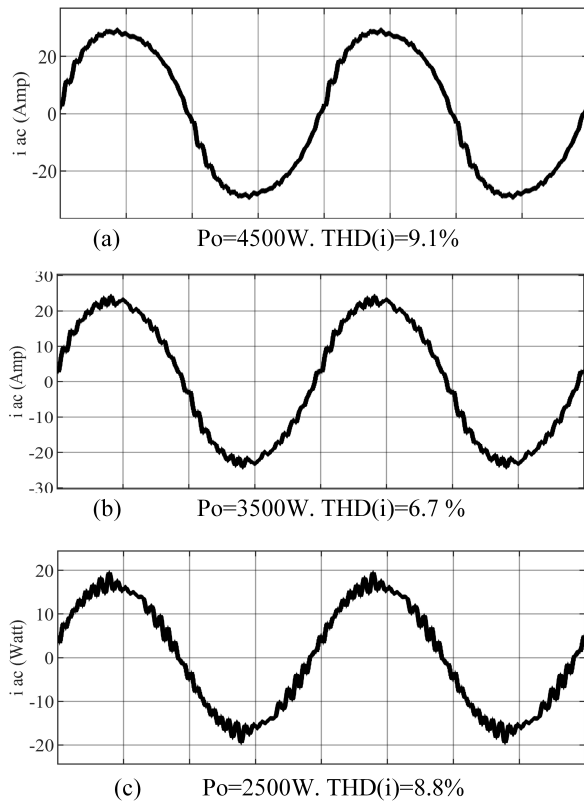


Fig. 8. Current for sinusoidal modulation function.

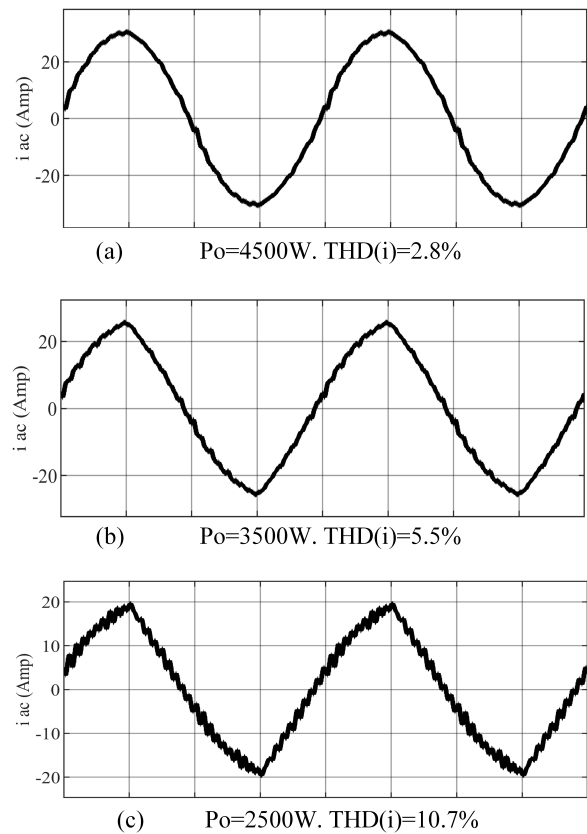


Fig. 9. Current for triangular modulation function.

maximum power by about 15% and 4% compared to sinusoidal and trigonometric modulation functions respectively. The variation of the power factor with k is shown in Fig. 12, it is shown that the power factor is 0.95 or higher for the three methods. The variation of THD with k shown in Fig. 13 depicts the main advantage of the proposed mPSM where it has the smallest distortion over the entire operation range. The results shown in Fig. 13 also show that the sinusoidal modulation causes large distortion for large values of k while the triangular modulation causes large distortion for small values of k and this result agrees with the the analysis presented in Section III. Over the entire range of k , the mPSM suggested in this paper reduces the THD by 55% and 39% respectively.

Table III describes the compliance to the requirements for current harmonic limits as described in IEEE Std- 19-2014 for the three methods [22]. It has been noticed that the sinusoidal modulation function fails to meet the standard due to low order harmonics distortion ($3 \leq n < 11$) for values of magnitude control ratio $k \geq 0.6$. For $k < 0.3$, the sinusoidal modulation function has large high frequency current ripple. The triangular modulation function meets the standard at large values of k but the high frequency ripple is excessive for $k < 0.5$. The proposed modified modulation scheme has no low frequency

ripple problem at high values of k but it acts almost as the sinusoidal function when $k < 0.3$.

V. CONCLUSION

A single-phase, one-stage, bidirectional, AC-DC power converter for use in electric micro-grids was subjected in this paper. The AC bridge is composed of four bidirectional switching modules. Considering phase shift modulation control, the effect of the modulation method on the AC current wave is analyzed for two basic modulation functions: the sinusoidal and the triangular. It is shown that the sinusoidal modulation function causes significant current distortion when the magnitude control ratio (k) is close to 1. The triangular modulation function has high distortion when k is small. The research suggests a new modified modulation function that leads to pure sinusoidal current over the entire range of k . Simulation study has been conducted to evaluate the performance of the three modulation methods. The results show that the proposed method has the advantage of linear relationship between k and the power besides lower harmonic distortion. The current distortion variation of the three methods in general

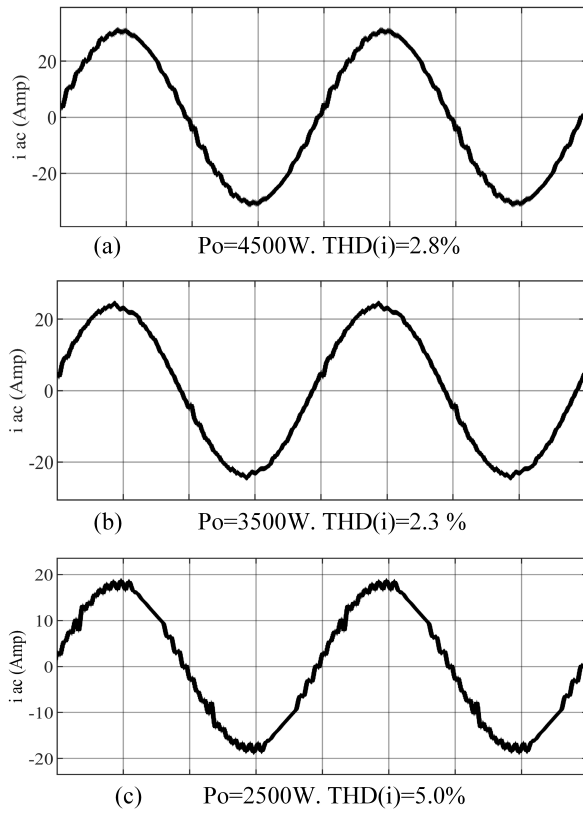


Fig. 10. Current for mPSM.

agrees with the analytical evaluation, however. due to the limitations of the LC filter at the AC side current incurs some distortion appears at low values of k . Nevertheless, the proposed method demonstrated a considerable reduction of 55% and 39% of harmonic distortion compared to sinusoidal and triangular modulation functions respectively. The proposed mPSM limits the maximum power transfer capability to 85% and 96% of the maximum power transferable using sinusoidal and triangular modulation functions respectively.

TABLE III.
CURRENT HARMONICS COMPARED TO IEEE STD 519.

| Modulation Method | Abiding range | Low order harmonics problem range | High order harmonics problem range |
|-------------------|-----------------|-----------------------------------|------------------------------------|
| Sinusoidal | $0.3 < k < 0.6$ | $0.6 < k < 1$ | $0 < k < 0.3$ |
| Triangular | $0.5 < k < 1$ | - | $0 < k < 0.5$ |
| Modified | $0.3 < k < 1$ | - | $0 < k < 0.3$ |

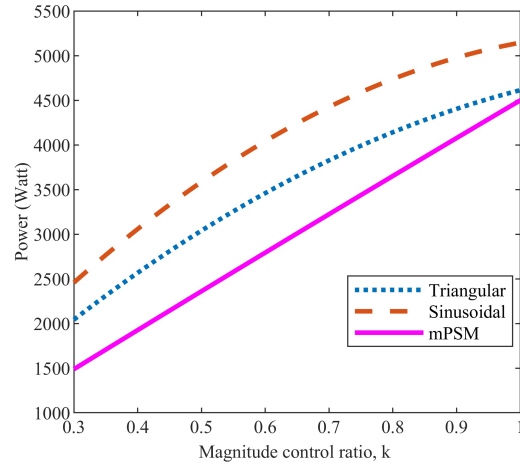


Fig. 11. The variation of the power with k .

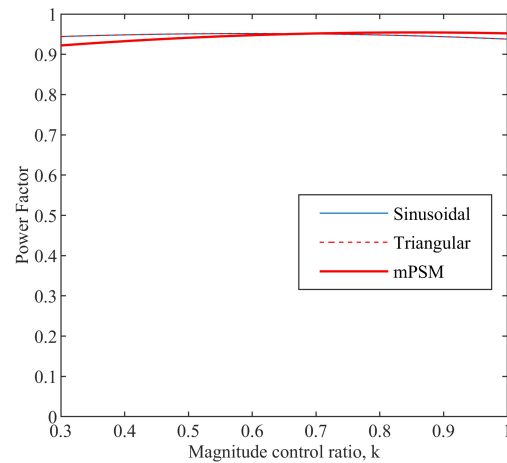


Fig. 12. The variation of the power factor with k .

CONFLICT OF INTEREST

The authors have no conflict of relevant interest to this article.

REFERENCES

[1] N. D. Weise, G. Castelino, K. Basu, and N. Mohan, "A single-stage dual-active-bridge-based soft switched ac-dc converter with open-loop power factor correction and other advanced features," *IEEE Transactions on Power Electronics*, vol. 29, no. 8, pp. 4007–4016, 2013.

[2] S. Zengin and M. Boztepe, "Loss analysis of trapezoid and triangular current modulated dcm ac/dc dab converter," in *2016 International Symposium on Fundamentals of Electrical Engineering (ISFEE)*, pp. 1–5, IEEE, 2016.

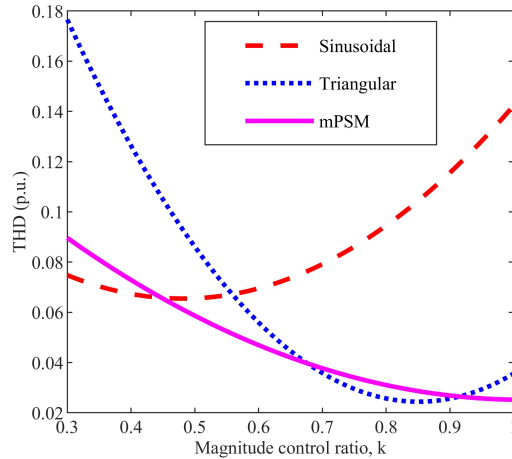


Fig. 13. The variation of (THD) with k .

- [3] J. M. Carrasco, L. G. Franquelo, J. T. Bialasiewicz, E. Galván, R. C. PortilloGuisado, M. M. Prats, J. I. León, and N. Moreno-Alfonso, "Power-electronic systems for the grid integration of renewable energy sources: A survey," *IEEE Transactions on industrial electronics*, vol. 53, no. 4, pp. 1002–1016, 2006.
- [4] X. Liang, "Emerging power quality challenges due to integration of renewable energy sources," *IEEE Transactions on Industry Applications*, vol. 53, no. 2, pp. 855–866, 2016.
- [5] A. Hameed, A. Nauman, M. Quadir, I. L. Khan, A. Iqbal, R. Hussain, and T. Khurshaid, "Advanced modulation scheme of a dual-active-bridge series resonant converter (dabsrc) for enhanced performance," *Mathematics*, vol. 10, no. 23, p. 4402, 2022.
- [6] J. Hiltunen, V. Väisänen, R. Juntunen, and P. Silventoinen, "Variable-frequency phase shift modulation of a dual active bridge converter," *IEEE Transactions on Power Electronics*, vol. 30, no. 12, pp. 7138–7148, 2015.
- [7] H. Kakigano, M. Nomura, and T. Ise, "Loss evaluation of dc distribution for residential houses compared with ac system," in *The 2010 International Power Electronics Conference-ECCE ASIA-*, pp. 480–486, IEEE, 2010.
- [8] R. W. De Doncker, D. M. Divan, and M. H. Kheraluwala, "A three-phase soft-switched high-power-density dc/dc converter for high-power applications," *IEEE transactions on industry applications*, vol. 27, no. 1, pp. 63–73, 1991.
- [9] M. Moonem and H. Krishnaswami, "Analysis of dual active bridge based power electronic transformer as a three-phase inverter," in *IECON 2012-38th Annual Conference on IEEE Industrial Electronics Society*, pp. 238–243, IEEE, 2012.
- [10] X. She, A. Q. Huang, and R. Burgos, "Review of solid-state transformer technologies and their application in power distribution systems," *IEEE journal of emerging and selected topics in power electronics*, vol. 1, no. 3, pp. 186–198, 2013.
- [11] J. Everts, "Closed-form solution for efficient zvs modulation of dab converters," *IEEE transactions on Power Electronics*, vol. 32, no. 10, pp. 7561–7576, 2016.
- [12] J. E. Huber and J. W. Kolar, "Volume/weight/cost comparison of a 1mva 10 kv/400 v solid-state against a conventional low-frequency distribution transformer," in *2014 IEEE Energy Conversion Congress and Exposition (ECCE)*, pp. 4545–4552, IEEE, 2014.
- [13] G. Castelino, K. Basu, and N. Mohan, "A novel three-phase bi-directional, isolated, single-stage, dab-based ac-dc converter with open-loop power factor correction," in *2012 IEEE International Conference on Power Electronics, Drives and Energy Systems (PEDES)*, pp. 1–6, IEEE, 2012.
- [14] F. Jauch and J. Biela, "Combined phase-shift and frequency modulation of a dual-active-bridge ac-dc converter with pfc," *IEEE Transactions on Power Electronics*, vol. 31, no. 12, pp. 8387–8397, 2016.
- [15] M. Wang, Q. Huang, S. Guo, X. Yu, W. Yu, and A. Q. Huang, "Soft-switched modulation techniques for an isolated bidirectional dc-ac," *IEEE Transactions on Power Electronics*, vol. 33, no. 1, pp. 137–150, 2017.
- [16] K. Vangen, T. Melaa, S. Bergsmark, and R. Nilsen, "Efficient high-frequency soft-switched power converter with signal processor control," in *[Proceedings] Thirteenth International Telecommunications Energy Conference-INTELEC 91*, pp. 631–639, IEEE, 1991.
- [17] J. E. Bosso, G. G. Oggier, and G. O. García, "Topología de transformador de estado sólido cc-ca trifásico de una sola etapa," in *2014 IEEE Biennial Congress of Argentina (ARGENCON)*, pp. 387–392, IEEE, 2014.
- [18] H.-S. Kim, M.-H. Ryu, J.-W. Baek, and J.-H. Jung, "High-efficiency isolated bidirectional ac-dc converter for a dc distribution system," *IEEE transactions on Power Electronics*, vol. 28, no. 4, pp. 1642–1654, 2012.

- [19] M. Llomplat, J. E. Bosso, R. E. Carballo, and G. O. García, “Novel modified phase-shift modulation strategy for isolated ac–dc power converters,” *IET Power Electronics*, vol. 13, no. 5, pp. 1022–1032, 2020.
- [20] B. Zhao, Q. Song, and W. Liu, “Power characterization of isolated bidirectional dual-active-bridge dc–dc converter with dual-phase-shift control,” *IEEE Transactions on Power Electronics*, vol. 27, no. 9, pp. 4172–4176, 2012.
- [21] R. Baranwal, G. F. Castelino, K. Iyer, K. Basu, and N. Mohan, “A dual-active-bridge-based single-phase ac to dc power electronic transformer with advanced features,” *IEEE Transactions on Power Electronics*, vol. 33, no. 1, pp. 313–331, 2017.
- [22] I. Power and E. Society, “Ieee recommended practice and requirements for harmonic control in electric power systems,” *New York, NY, USA*, pp. 1–1, 2014.